Magnetoelastic coupling in magnetically frustrated $Co_3V_2O_8$

L. I. Vergara,[1] J. Cao,[1] L.-C. Tung,[2] N. Rogado,[3] F. Yen,[4,*] Y. Q. Wang,[4] R. J. Cava,[3] B. Lorenz,[4] Y.-J. Wang,[2] and J. L. Musfeldt[1]

[1]*Department of Chemistry, University of Tennessee, Knoxville, Tennessee 37996, USA*

[2]*National High Magnetic Field Laboratory, Tallahassee, Florida 32310, USA*

[3]*Department of Chemistry and Princeton Materials Institute, Princeton University, Princeton, New Jersey 08544, USA*

[4]*Department of Physics and TCSUH, University of Houston, Houston, Texas 77204, USA*

(Received 5 November 2009; published 15 January 2010)

An applied magnetic field offers the opportunity to drive new transitions and tune competing interactions in complex materials. Here, we employ magnetoinfrared spectroscopy to probe magnetic ordering-induced local lattice distortions through the series of field-induced transitions in the frustrated Kagomé staircase material $Co_3V_2O_8$. These experiments reveal that the most important local lattice distortion involves Co center displacement, mainly along the direction perpendicular to the buckled Kagomé planes. This result is important for understanding the microscopic aspects of magnetically driven transitions in functional oxides.

DOI: 10.1103/PhysRevB.81.012403 PACS number(s): 75.50.Cc, 63.20.−e, 75.25.−j, 75.30.Et

The interplay between charge, structure, and magnetism is the physical basis for many of the unique properties of complex materials. In magnetic systems, for instance, functionality is determined by low-energy scale spin-interaction processes such as exchange, anisotropy, and frustration that sometimes appear in combination with higher energy processes such as magnetoelastic coupling. Recent investigations reveal strong evidence for lattice flexibility in coupled systems[1–8] although the microscopic aspects of these interactions and the effect of magnetic field on local structure are not well established. This is because direct observation of field-dependent phonons is quite rare, and as a consequence, there are few physical systems with which to evaluate specific changes in bond lengths and angles that accompany magnetic transitions. As a candidate for a frustrated solid that can exhibit substantial magnetoelastic coupling, we consider the Kagomé staircase material $Co_3V_2O_8$ (Refs. 9–11) and employ high-field vibrational spectroscopy to evaluate magnetic ordering-induced local lattice distortions.

$Co_3V_2O_8$ displays an orthorhombic crystal structure with Kagomé-like layers of edge-sharing CoO_6 octahedra separated by VO_4 tetrahedra.[12] Here, the Co^{2+} centers are $S=3/2$, whereas V^{5+} is d^0 and nonmagnetic. Unlike the ideal Kagomé net, there are two crystallographically inequivalent magnetic sites abbreviated here as Co_s and Co_c to indicate spine and crosstie sites, respectively. The spine sites form chains along a and are linked by the crosstie sites in the c direction to form a buckled Kagomé staircase. These planes are stacked along b to complete the structure. The rich magnetic field-temperature phase diagram is a consequence of magnetic frustration.[9,10,13,14] At ~4 K and zero field, $Co_3V_2O_8$ displays a weakly ferromagnetic (w-FM) ground state. Here, Co_s moments align parallel to the a axis with an amplitude of $\sim 3.0\mu_B$.[9,10] Co_c sites show ordered moments of $\sim 1.9\mu_B$, with alignment either along a (Ref. 9) or ~10° toward c from a.[10] Inelastic neutron scattering combined with spin-wave theory demonstrates that magnetic coupling is predominantly between spine and crosstie sites.[15] An applied magnetic field stabilizes a series of new states, summarized schematically in Fig. 1(a) for the case of an isotropic sample like ours. Between 1 and 2 T, $Co_3V_2O_8$ shows a re-entrant transition from w-FM into the incommensurate antiferromagnetic (IC-AFM) state, and back to the w-FM state ($H \| c$).[10,13,14] Near 4 T, there are two transitions depending on the field direction: the w-FM→paramagnetic (PM) transition for $H \| c$,[9,10,13,14] and the w-FM→IC-AFM transition for $H \| b$.[14] In the IC-AFM phase, Co_s spins participate in a transversely polarized spin-density wave. The wave vector is along b and the moments are directed along a. Two models are again proposed for the Co_c moments, with alignment either along a (Ref. 9) or mostly along the a axis with a ~10° cant toward c.[10] An IC-AFM→PM transition appears between 8 and 12 T for $H \| b$.[10,14] Ferroelectricity has not been observed in $Co_3V_2O_8$,[9,10,13] different from quasi-isostructural $Ni_3V_2O_8$, which is a well-known magnetically driven multiferroic.[16]

In order to investigate magnetoelastic coupling in a frustrated Kagomé staircase material, we measured the magneto-infrared response of $Co_3V_2O_8$. Three vibrational modes (b_4, b_{11}, and c_8) are sensitive to the series of field-induced transitions; changes in b_4 are substantial. Combining field-induced frequency shifts and area changes with calculated displacement patterns,[17,18] we evaluate the local lattice distortions. We find that local structure changes between the w-FM and PM states involve Co center displacements and "squashing" of the octahedron, changes that modify superexchange interactions and dovetail with thermal expansion studies.[9–11]

Our samples were prepared by mixing small pieces of $Co_3V_2O_8$ broken from larger crystals with paraffin or KCl powder to form isotropic pellets for far and middle infrared, respectively. The use of randomly oriented crystallites implies a continuous distribution of the applied magnetic field with respect to one particular axis in different crystallites, but it offers advantageous control of composition and simultaneous investigation of all field directions. Magnetoinfrared transmittance experiments were carried out at 4.2 K using a Bruker 66v/S Fourier transform infrared spectrometer and an 18 T magnet. The absorption coefficient was calculated as $\alpha(\omega,H) = -(1/hd)\ln \mathcal{T}(\omega,H)$, where h is the loading, d is the thickness, and $\mathcal{T}(\omega,H)$ is the measured transmittance. To emphasize changes with

 ©2010 The American Physical Society

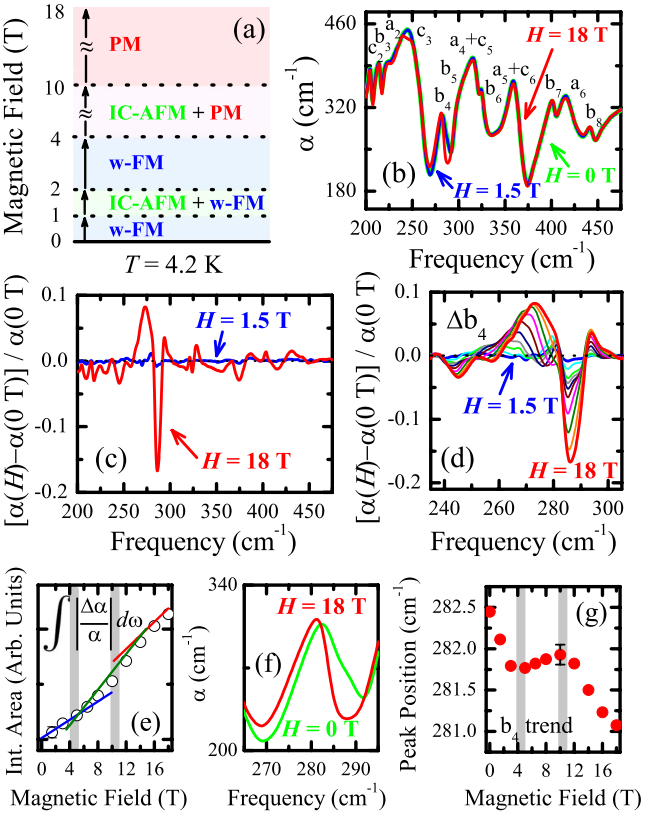

FIG. 1. (Color online) (a) Schematic H-T phase diagram for $Co_3V_2O_8$ at 4.2 K, combining results for the three crystallographic directions (Refs. 9, 10, 13, and 14); (b) absolute absorption spectra of $Co_3V_2O_8$ at 4.2 K in the low-frequency range for 0, 1.5, and 18 T; (c) absorption difference spectra $[\alpha(H)-\alpha(0\ \mathrm{T})]/\alpha(0\ \mathrm{T})$ calculated from spectra shown in (b); (d) close-up view of the absorption difference spectra of $Co_3V_2O_8$ near 280 cm^{-1}. The data are shown for H=1.5, 3, 5, 6.5, 8, 10, 12, 14, 16, and 18 T; (e) integrated area in arbitrary units, the solid straight lines show trend changes; (f) close-up view of the b_4 absorption for 0 and 18 T; and (g) frequency shift of the b_4 peak in the absolute absorption spectra as a function of applied magnetic field. In (e) and (g), the gray vertical lines highlight positions of possible magnetic phase boundaries.

magnetic field, we also calculated the absorption difference spectra $[\alpha(\omega,H)-\alpha(\omega,0\ \mathrm{T})]/\alpha(\omega,0\ \mathrm{T})$. One way to quantify field-induced changes in the absorption difference is through $\int_{\omega_0}^{\omega_1}\left|\frac{\alpha(\omega,H)-\alpha(\omega,0\ \mathrm{T})}{\alpha(\omega,0\ \mathrm{T})}\right|d\omega$, where ω_0 and ω_1 define the frequency range of interest. This provides a measure of contrast associated with a particular mode.

Figure 1(b) displays the absolute absorption spectrum of $Co_3V_2O_8$ at 4.2 K at different magnetic fields. We relied on existing first-principles calculations of frequency and displacement patterns along with the nomenclature in Refs. 17 and 18 and zero-field single crystal results to identify and label the spectral features. To emphasize field-induced effects, we calculate the absorption difference spectra $[\alpha(\omega,H)-\alpha(\omega,0\ \mathrm{T})]/\alpha(\omega,0\ \mathrm{T})$, from which we can see that several modes change systematically with magnetic field. These changes are on the order of few percent, with a complex derivativelike structure indicative of frequency and linewidth shifts. The largest effect is near 280 cm^{-1} [Fig. 1(c)]. We assign this signature in the absorption difference spectrum to a modification of the b_4 mode. The latter has B_{2u} symmetry and involves Co_s motion along b plus diagonal Co_c motion along $b+c$ [Fig. 2(a)].[17,18] The peak-to-dip change in the absorption difference spectrum is ~25% at 18 T, large compared to Mn_{12}-acetate,[6] κ−$(ET)_2Cu[N(CN)_2]Br$,[7] and similar results on $Ni_3V_2O_8$ (~3% change in b_4 at 18 T).

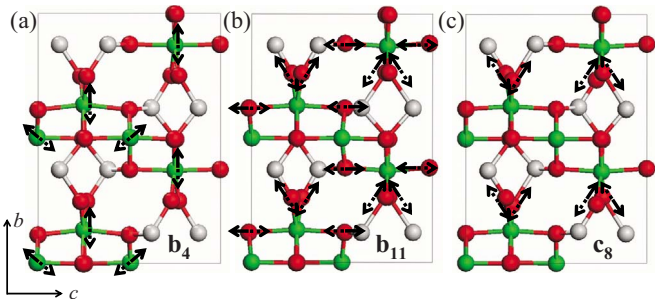

FIG. 2. (Color online) Schematic representation of the calculated b_4, b_{11}, and c_8 displacement patterns in the bc plane (Refs. 17 and 18). Here, green=Co^{2+} (medium), red=O^{2-} (dark), and grey =V^{5+} (light).

Figure 1(d) displays a close-up view of the absorption difference data in the vicinity of the b_4 mode. Slope changes in the integrated absorption difference spectra [Fig. 1(e)] are observed near 4 and 10 T. Frequency shifts are best quantified directly from the absolute absorption response [Figs. 1(f) and 1(g)]. With increasing field, b_4 softens toward ~4 T, hardens slightly until ~10 T, and softens again up to 18 T. As discussed below, these changes correlate with critical fields.

The magnetic field-temperature phase diagram of $Co_3V_2O_8$ displays a series of transitions with applied field.[9,10,13,14] An isotropic sample such as ours provides only superimposed rather than directional results. Nevertheless, useful information can be obtained.[19] The w-FM→IC-AFM→w-FM re-entrant transition near 1.5 T ($H\|c$) (Refs. 10, 13, and 14) does not affect the phonons within our sensitivity. We therefore conclude that the lattice is not sensitive to the IC-AFM state. Both frequency and integrated area changes in b_4 are observed near 4 T. Comparing with the phase diagram [Fig. 1(a)], these changes can be attributed to the w-FM→PM transition ($H\|c$),[9,10,13,14] the w-FM→IC-AFM transition ($H\|b$),[14] or a combination of the two. The lack of clear phonon anomalies near 1.5 T argues for assignment of the 4 T frequency shift and oscillator strength changes in b_4 as signatures of the w-FM→PM transition. In other words, b_4 is sensitive to the transition from the long-range ordered state into the short-range fully polarized state. We assign slope changes in the frequency shift and integrated area data at ~10 T to the IC-AFM→PM transition ($H\|b$) as reported by Wilson *et al.*[14] Extrapolation of data by Yasui *et al.*[10] and Yen *et al.*[13] to higher magnetic fields for $H\|b$ supports this assignment. Again, b_4 is sensitive to the PM state.

Figure 3(a) displays the magnetoinfrared response of $Co_3V_2O_8$ in the high-frequency regime. As before, peak assignments were carried out based on existing first-principles

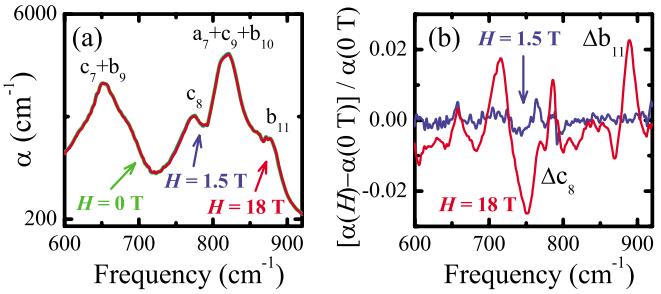

FIG. 3. (Color online) (a) Absolute absorption spectra of $Co_3V_2O_8$ at 4.2 K in the high-frequency range for 0, 1.5, and 18 T. (b) Absorption difference spectra $[\alpha(H)-\alpha(0\ \mathrm{T})]/\alpha(0\ \mathrm{T})$ calculated from spectra shown in (a).

calculations for $Ni_3V_2O_8$.[17,18] The absorption difference spectrum [Fig. 3(b)] reveals that several other modes show field dependence, although the effects are much smaller than those of the b_4 mode. These include a combination of peaks near 730 cm^{-1} and the ~880 cm^{-1} feature. We assign field-induced spectral changes at 880 cm^{-1} to modifications of the b_{11} mode. It has B_{2u} symmetry and involves only oxygen centers in the VO_4 asymmetric stretch. On the other hand, changes near 730 cm^{-1} are due to combined effects. This is because the tail of c_7+b_9 overlaps with the leading edge of c_8 and $a_7+c_9+b_{10}$. In spite of this complicated superposition, we successfully extracted field trends in the c_8 mode. Schematic views of the displacement patterns for b_{11} and c_8 are shown in Figs. 2(b) and 2(c).[17,18]

Figure 4(a) displays a close-up view of the absorption difference data for the b_{11} mode. The field-induced spectral modifications become noticeable only above 4 or 5 T, again indicating that the 1.5 T w-FM→IC-AFM→w-FM reentrant transition does not affect the phonons significantly. Above 4 or 5 T, the contrast increases systematically with applied field. At 18 T, a peak-to-dip change of 3% is observed. Figure 4(b) shows the integrated absorption difference spectra for b_{11}. The sharp increase above 4 T plus the slope change at higher field demonstrate the sensitivity of b_{11} to the PM state.

We can also quantify changes in the c_8 mode near 775 cm^{-1} [Figs. 4(c) and 4(d)]. For this analysis, we account for the comparatively flat absorption difference spectrum between 800 and 850 cm^{-1} and disregard the field effect on the

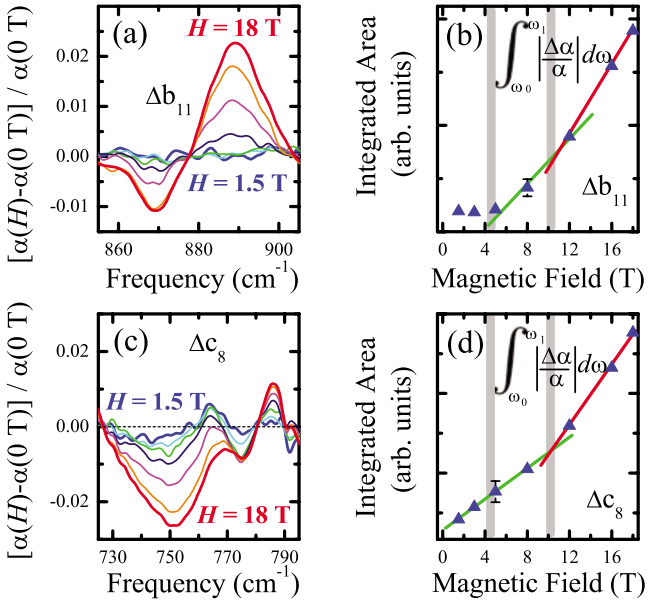

FIG. 4. (Color online) (a) Close-up view of the absorption difference spectra of $Co_3V_2O_8$ near 880 cm^{-1}; (b) integrated area of Δb_{11} as a function of applied magnetic field; (c) close-up view of the difference absorption spectra for the c_8 mode at different applied fields; and (d) integrated area of Δc_8 as a function of applied magnetic field. In (a) and (c), the data are shown for H=1.5, 3, 5, 8, 12, 16, and 18 T. In (b) and (d), the straight lines highlight trend changes, and the gray vertical lines indicate possible magnetic phase boundaries.

c_7+b_9 tail. Both actions were required in order to isolate this effect from other nearly superimposed features.[20] Figure 4(d) displays the integrated absorption difference spectrum. No changes are observed near 1.5 or 4 T, indicating that the c_8 mode is not involved in either of these transitions. There is, however, a slope change near 10 T. We associate this slope change with the IC-AFM→PM transition ($H\|b$).

Table I summarizes our findings. Modifications to the b_4 mode are the most important magnetoelastic effect. That said, it is quite natural that other lattice relaxation channels (as represented by the b_{11} and c_8 modes) are needed to accommodate dominant b_4 mode coupling to the magnetic transitions in this extended system.

We can combine the aforementioned trends with an analy-

TABLE I. Summary of properties for the three field-dependent modes. Columns provide: mode label, frequency in cm^{-1}, description of motion, displacement of Co centers, superexchange modification, sensitivity to magnetic phase transitions, and absorption difference change at full field.

Mode label	Frequency (cm^{-1})	Simple sketch	Co displacement	Superexchange	Magnetic transition	Change at 18 T (%)
b_4	280	Mix of O-V-O and O-Co-O bend	Co_s: b Co_c: $b+c$	Co_s-O-Co_s Co_s-O-Co_c	~4 T w-FM→PM ~10 T IC-AFM→PM	25
b_{11}	880	V-O stretch + O-Co-O bend	No	Co_s-O-Co_s Co_s-O-Co_c	~4 T w-FM→PM ~10 T IC-AFM→PM	3
c_8	775	V-O stretch + O-Co-O bend	No	Co_s-O-Co_s	~10 T IC-AFM→PM	3

sis of mode displacement patterns[17,18] to reveal the local lattice distortion in the high-field PM state compared to that in the zero-field w-FM state. This analysis relies on the fact that each magnetic state can (in principle) have its own local structure and unique vibrational characteristics. The overall softening of b_4 through the field-driven w-FM→PM transition [Fig. 1(g)] is indicative of a relaxation involving the Co centers. Specifically, it points toward Co_s displacement along b and Co_c displacement along $b+c$. These shifts modify the local polyhedral environment and associated superexchange interactions. On the other hand, b_{11} and c_8 are very simple vibrational modes involving O motion along the V-O bonds.[21] These much smaller changes in the oxygen framework modify the CoO_6 environment and act to accommodate the Co center relaxations mandated by b_4. They also affect associated superexchange interactions. This scenario of shifted Co centers and "squashed" polyhedra through the w-FM→PM transition is in line with the overall b-axis expansion and c-axis contraction found in thermal-expansion measurements.[9–11]

These trends allow us to consider structure-property relationships in the $M_3V_2O_8$ family of materials (M=transition metal). In multiferroic $Ni_3V_2O_8$, the b_4 vibrational mode softens considerably in the low-temperature incommensurate state.[22] Here, the b_4 mode breaks inversion symmetry and creates the distortion that establishes the spontaneous b-directed ferroelectric polarization.[16–18] That the same mode shows heightened sensitivity to applied field in $Co_3V_2O_8$ demonstrates its importance in this family of quasi-isostructural Kagomé staircase materials, although large changes in b_4 clearly do not by themselves correlate with multiferroicity. Using this spectral data, we can also estimate the change in the static dielectric constant of $Co_3V_2O_8$ with field. We find that $\Delta\epsilon_1$ is small at 5 or 7 T in agreement with literature results;[13,23] $\Delta\epsilon_1$ is −0.01 at 18 T.

Summarizing, we employed vibrational spectroscopy to investigate magnetoelastic coupling and local lattice distortions in magnetically frustrated $Co_3V_2O_8$. The b_4 mode, which involves Co center displacements, displays a particularly strong magnetoinfrared effect that when analyzed with calculated displacement patterns reveals the microscopic aspects of the field-induced local lattice distortion. This result is important for other magnetically frustrated oxides where magnetic-ordering-induced lattice distortions are also likely to occur.

This work is supported by the U.S. Department of Energy (UT, Princeton, NHMFL), National Science Foundation (NHMFL), the State of Florida (NHMFL), and the State of Texas (TCSUH). We thank G. Lawes for useful conversations.

*Present address: Southwest Jiaotong University, Chengdu, Sichuan 610031, China.

[1] B. García-Landa, C. Marquina, M. R. Ibarra, G. Balakrishnan, M. R. Lees, and D. McK. Paul, Phys. Rev. Lett. **84**, 995 (2000).
[2] A. N. Lavrov, S. Komiya, and Y. Ando, Nature (London) **418**, 385 (2002).
[3] S. E. Russek, P. Kabos, R. D. McMichael, C. G. Lee, W. E. Bailey, R. Ewasko, and S. C. Sanders, J. Appl. Phys. **91**, 8659 (2002).
[4] V. S. Zapf, V. F. Correa, P. Sengupta, C. D. Batista, M. Tsukamoto, N. Kawashima, P. Egan, C. Pantea, A. Migliori, J. B. Betts, M. Jaime, and A. Paduan-Filho, Phys. Rev. B **77**, 020404(R) (2008).
[5] T. Ruf, C. Thomsen, R. Liu, and M. Cardona, Phys. Rev. B **38**, 11985 (1988).
[6] A. B. Sushkov, J. L. Musfeldt, Y. J. Wang, R. M. Achey, and N. S. Dalal, Phys. Rev. B **66**, 144430 (2002).
[7] R. Wesołowski, J. T. Haraldsen, J. Cao, J. L. Musfeldt, I. Olejniczak, J. Choi, Y. J. Wang, and J. A. Schlueter, Phys. Rev. B **71**, 214514 (2005).
[8] J. Cao, L. I. Vergara, J. L. Musfeldt, A. P. Litvinchuk, Y.-J. Wang, S. Park, and S.-W. Cheong, Phys. Rev. Lett. **100**, 177205 (2008).
[9] Y. Chen, J. W. Lynn, Q. Huang, F. M. Woodward, T. Yildirim, G. Lawes, A. P. Ramirez, N. Rogado, R. J. Cava, A. Aharony, O. Entin-Wohlman, and A. B. Harris, Phys. Rev. B **74**, 014430 (2006).
[10] Y. Yasui, Y. Kobayashi, M. Soda, T. Moyoshi, M. Sato, N. Igawa, and K. Kakurai, J. Phys. Soc. Jpn. **76**, 034706 (2007).
[11] Y. Kobayashi, Y. Yasui, and M. Sato, J. Magn. Magn. Mater. **310**, 1160 (2007).
[12] E. E. Sauerbrei, R. Faggiani, and C. Calvo, Acta Crystallogr., Sect. B: Struct. Crystallogr. Cryst. Chem. **29**, 2304 (1973).
[13] F. Yen, R. P. Chaudhury, E. Galstyan, B. Lorenz, Y. Q. Wang, Y. Y. Sun, and C. W. Chu, Physica B **403**, 1487 (2008).
[14] N. R. Wilson, O. A. Petrenko, and G. Balakrishnan, J. Phys.: Condens. Matter **19**, 145257 (2007).
[15] M. Ramazanoglu, C. P. Adams, J. P. Clancy, A. J. Berlinsky, Z. Yamani, R. Szymczak, H. Szymczak, J. Fink-Finowicki, and B. D. Gaulin, Phys. Rev. B **79**, 024417 (2009).
[16] G. Lawes, A. B. Harris, T. Kimura, N. Rogado, R. J. Cava, A. Aharony, O. Entin-Wohlman, T. Yildirim, M. Kenzelmann, C. Broholm, and A. P. Ramirez, Phys. Rev. Lett. **95**, 087205 (2005).
[17] A. B. Harris, T. Yildirim, A. Aharony, and O. Entin-Wohlman, Phys. Rev. B **73**, 184433 (2006).
[18] T. Yildirim, L. I. Vergara, J. Íñiguez, J. L. Musfeldt, A. B. Harris, N. Rogado, R. J. Cava, F. Yen, R. P. Chaudhury, and B. Lorenz, J. Phys.: Condens. Matter **20**, 434214 (2008).
[19] The fact that we observe relatively sharp anomalies despite the random grain orientation indicates that the true nature of these anomalies should be even sharper and more pronounced in a single crystal with perfect alignment with respect to the field.
[20] With these assumptions, we integrated the absorption difference between 720 and 800 cm^{-1}.
[21] Since all oxygen atoms are connected to Co centers, these modes cannot be described as purely V-O stretching because they are always mixed with some Co-O bond stretching or O-Co-O bending.
[22] L. I. Vergara, J. Cao, N. Rogado, Y. Q. Wang, R. P. Chaudhury, R. J. Cava, B. Lorenz, and J. L. Musfeldt, Phys. Rev. B **80**, 052303 (2009).
[23] N. Bellido, C. Martin, C. Simon, and A. Maignan, J. Phys.: Condens. Matter **19**, 056001 (2007).